

Topological Dimensions from Disorder and Quantum Mechanics?

Ivan Horváth ^{1,2,*} and Peter Markoš ³¹ Nuclear Physics Institute CAS, 25068 Řež near Prague, Czech Republic² Department of Physics and Astronomy, University of Kentucky, Lexington, KY 40506, USA³ Department of Experimental Physics, Faculty of Mathematics, Physics and Informatics, Comenius University in Bratislava, Mlynská Dolina 2, 842 28 Bratislava, Slovakia; peter.markos@fmph.uniba.sk

* Correspondence: ihorv2@g.uky.edu

Abstract: We have recently shown that the critical Anderson electron in $D = 3$ dimensions effectively occupies a spatial region of the infrared (IR) scaling dimension $d_{\text{IR}} \approx 8/3$. Here, we inquire about the dimensional substructure involved. We partition space into regions of equal quantum occurrence probabilities, such that the points comprising a region are of similar relevance, and calculate the IR scaling dimension d of each. This allows us to infer the probability density $p(d)$ for dimension d to be accessed by the electron. We find that $p(d)$ has a strong peak at d very close to two. In fact, our data suggest that $p(d)$ is non-zero on the interval $[d_{\text{min}}, d_{\text{max}}] \approx [4/3, 8/3]$ and may develop a discrete part (δ -function) at $d = 2$ in the infinite-volume limit. The latter invokes the possibility that a combination of quantum mechanics and pure disorder can lead to the emergence of integer (topological) dimensions. Although d_{IR} is based on effective counting, of which $p(d)$ has no a priori knowledge, $d_{\text{IR}} \geq d_{\text{max}}$ is an exact feature of the ensuing formalism. A possible connection of our results to the recent findings of $d_{\text{IR}} \approx 2$ in Dirac near-zero modes of thermal quantum chromodynamics is emphasized.

Keywords: Anderson transition; localization; effective counting dimension; effective number theory; effective support; dimension content; emergent space



Citation: Horváth, I.; Markoš, P. Topological Dimensions from Disorder and Quantum Mechanics? *Entropy* **2023**, *25*, 1557. <https://doi.org/10.3390/e25111557>

Academic Editors: Aimin Guo and Qiao Chen

Received: 16 October 2023
Revised: 10 November 2023
Accepted: 13 November 2023
Published: 17 November 2023



Copyright: © 2023 by the authors. Licensee MDPI, Basel, Switzerland. This article is an open access article distributed under the terms and conditions of the Creative Commons Attribution (CC BY) license (<https://creativecommons.org/licenses/by/4.0/>).

1. Introduction

Understanding the spatial geometry of Anderson transitions [1] is an intriguing problem. Indeed, although studied quite extensively, the complicated structure of critical electronic states (see e.g., [2]) leaves room for new insights. Novel characterization may reveal unknown details of disorder-driven metal-insulator transitions and, for example, lead to a deeper understanding of their renormalization group description [3].

Another reason to study the geometry of Anderson transitions arises by seeing them as quantum *dimension transitions*, a viewpoint taken in Ref. [4]. Using effective number theory (ENT) [5,6], which entails a unique measure-based dimension d_{IR} [7,8] for spaces with probabilities, it was shown there that the transition is a two-step dimension reduction

$$d_{\text{IR}} = 3 \longrightarrow \approx 8/3 \longrightarrow 0 \quad (1)$$

Here the flow is from the extended to critical to localized states, and exponential localization was assumed. A remarkable property of the above is that these reductions are complete [9]. Indeed, the probability does not leak away from subdimensional effective supports, and the electron is fully confined to them in infinite volume. It is thus meaningful to say that the space available to quantum particles collapses into a lower-dimensional one under the influence of strong enough disorder. As such, it represents a mechanism for generating lower-dimensional spaces by simple combination of quantum mechanics and disorder.

While dimension is the most basic characteristic of space available to a critical electron, this space may contain subsets with dimensions $d < d_{\text{IR}}$. Such a substructure may be

physically significant if electron mostly resides there. The aim of this work is to characterize the critical spatial geometry in such a manner: we will compute the probability distribution $p(d)$ that the electron is present in a space of dimension d . We refer to $p(d)$ as the *dimension content* of the Anderson criticality or that of the probability distribution in general.

Critical states at Anderson transitions were recognized to have fractal-like features long ago, first interpreting them in analogy to scale-invariant fractals [10,11] and, later, to more complex multifractals [12–15]. The formalism used in the latter mimics one that describes the ultraviolet (UV) measure singularities occurring in turbulence and strange attractors (see, e.g., [16,17]). More recent works in the Anderson context are [18–22]. However, the focus of multifractal analysis does not make it convenient for computing $p(d)$. We thus proceed by proposing a method that organizes the calculation in terms of probabilities from the outset and zooms in on dimensions by the degree of their actual presence. Moreover, the d involved is simply the IR Minkowski dimension of a subset and thus manifestly a measure-based dimension of space. In the ensuing multidimensionality formalism, a given wave function is

$$\begin{aligned}
 &\text{subdimensional if} && d_{\text{IR}} < D \\
 &\text{multidimensional if} && p(d) \neq \delta(d - d_{\text{max}}) \\
 &\text{of proper dimension if} && d_{\text{IR}} = d_{\text{max}}
 \end{aligned} \tag{2}$$

where $d_{\text{max}} = \sup \{d \mid p(d) > 0\}$, $D = 3$ is the IR dimension of the underlying space, and $d_{\text{IR}} \geq d_{\text{max}}$ holds in general.

Before proceeding to define $p(d)$, we illustrate the idea on a “shovel” in $\mathbb{R}^{D=3}$ space (Figure 1). The shovel consists of 2D square blade and 1D handle with the uniformly distributed masses $M_b > 0$ and $M_h > 0$, respectively. If the relevance of space points is set by the mass they carry, the probabilities of encountering the handle, the blade, and the rest of space are $\mathcal{P} = M_h / (M_b + M_h)$, $1 - \mathcal{P}$ and 0, respectively. Note that the UV cutoff a and IR cutoff L are also indicated.

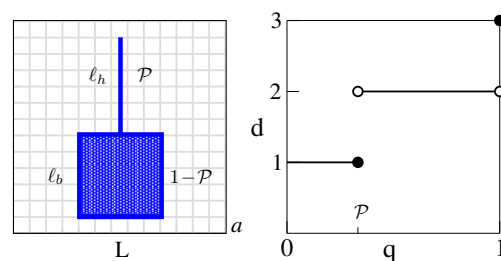


Figure 1. The “shovel” (left) and $d(q)$ (right) associated with its UV dimension content in \mathbb{R}^3 . See the discussion in the text.

Above, we implicitly assumed that d is the usual UV dimension ($a \rightarrow 0$ at a fixed L), in which case we have by inspection $p(d) = \mathcal{P} \delta(d - 1) + (1 - \mathcal{P}) \delta(d - 2)$. However, how would this $p(d)$ be concluded by a computer that cannot “see” and only processes regularized probability vectors $P(a) = (p_1, p_2, \dots, p_{N(a)})$? Here, $N(a) = (L/a)^3$, p_i is the probability within an elementary cube at the point x_i of a latticized space, and $a \in \{L/k \mid k = 2, 3, \dots\}$.

Anticipating that any number J of discrete dimensions $0 \leq d_1 < d_2 < \dots < d_J \leq 3$ with probabilities $\mathcal{P}_j > 0$ could be present, the computer first orders p_i in each $P(a)$ so that $p_1 \geq p_2 \geq \dots \geq p_{N(a)}$. The rationale is that, with decreasing a , this increasingly better separates out populations related to a different d_j . Indeed, the typical size of p associated with d_j is $\propto a^{d_j}$ and so $P(a)$ gradually organizes into J sequential blocks starting with d_1 . The above ordering in P will always be assumed from now on.

To detect possible blocks/dimensions, the computer uses the variable $q \in [0, 1]$ for cumulative probability, and associates with each $P(a)$ the function $v(q, a)$, namely the number of first elements in $P(a)$ (space points) whose probabilities add up to q . Keeping track of the fractional boundary contributions at each q makes it a continuous, convex,

increasing, piecewise linear function such that $v(0, a) = 0$ and $v(1, a) = N(a)$. The number of points in the interval $(q - \epsilon, q]$ is $v(q, a) - v(q - \epsilon, a)$ and scales as $a^{-d(q, \epsilon)}$ for $a \rightarrow 0$. When processing $P(a)$ for the shovel, the computer finds perfect scaling $(\ell_h/a) \times \epsilon/\mathcal{P}$ for $\epsilon \leq q \leq \mathcal{P}$, and $(\ell_b/a)^2 \times \epsilon/(1 - \mathcal{P})$ for $\mathcal{P} + \epsilon < q < 1$. It will thus conclude $d(q)$ shown in Figure 1 upon $\epsilon \rightarrow 0$. The value at $q = 1$ represents the spatial complement of the shovel (zero probability). Collecting the probability of d , namely $p(d) = \int_0^1 dq \delta(d - d(q))$, produces the inspected result.

Two points are relevant here. (1) The above approach does not change if a continuous set of dimensions is present. In this case the obtained $d(q)$ is not piecewise-constant but rather a piecewise-continuous, non-decreasing function, possibly with constant parts identifying discrete dimensions. (2) The IR case is fully analogous, but it is useful to recall the meaning of the IR dimension ($L \rightarrow \infty$, a fixed) which is somewhat non-standard. Thus, if both ℓ_h and ℓ_b are fixed as $L \rightarrow \infty$ (the usual case), then $p(d) = \delta(d)$ since the populations at each q remain constant. However, if e.g. ℓ_b is fixed while the handle responds by $\ell_h \propto L$ (the shovel reaches anywhere in space), then $p(d) = (1 - \mathcal{P})\delta(d) + \mathcal{P}\delta(d - 1)$.

2. The Formalism

We now define $p(d)$ in the IR setting of the Anderson transitions. Such analysis pertains to the wave functions $\psi = \psi(r_i)$ on a cubic lattice of $N(L) = (L/a)^D$ sites r_i , with L the IR regulator and a set to unity. With ψ , we associate the probability vector $P = (p_1, p_2, \dots, p_{N=N(L)})$, where $p_i = \psi^\dagger \psi(r_i)$, the effective number of sites [5,6]

$$\mathcal{N}_*[\psi] = \sum_{i=1}^N n_*(Np_i) \quad , \quad n_*(c) = \min\{c, 1\} \tag{3}$$

and the cumulative count $v[q, \psi]$ defined as follows. Consider the cumulative probabilities (q_0, q_1, \dots, q_N) with $q_0 = 0$ and $q_j = \sum_{i=1}^j p(i)$ for $j > 0$. Let $j(q)$, $q \in (0, 1)$ be the largest j such that $q_j < q$. Then $v[0, \psi] = 0$, $v[1, \psi] = N$ and

$$v[q, \psi] = j(q) + \frac{q - q_j}{q_{j+1} - q_j} \quad , \quad 0 < q < 1 \tag{4}$$

Recalling the order in P , $v[q, \psi]$ is increasing and convex.

Consider the Anderson model in the orthogonal class [1]. With c_{r_i} , the electron operators, the Hamiltonian is

$$\mathcal{H} = \sum_i \epsilon_{r_i} c_{r_i}^\dagger c_{r_i} + \sum_{i,j} c_{r_i}^\dagger c_{r_i - e_j} + h.c. \tag{5}$$

where e_j ($j = 1, \dots, D$) are unit lattice vectors and random potentials $\epsilon_{r_i} \in [-W/2, +W/2]$ are uniformly distributed. The physics of the model involves averaging over disorder $\{\epsilon_{r_i}\}$. For \mathcal{N}_* and v of one-particle eigenstates ψ at an energy E , we have

$$\mathcal{N}_*[\psi] \rightarrow \mathcal{N}_*(E, W, L) \quad , \quad v[q, \psi] \rightarrow v(q, E, W, L) \tag{6}$$

Keeping the dependence on E and W implicit, the $L \rightarrow \infty$ behavior defines the dimensional characteristics d_{IR} and $d(q)$ via

$$\mathcal{N}_*(L) \propto L^{d_{\text{IR}}} \quad , \quad v(q, L) - v(q - \epsilon, L) \propto L^{d(q, \epsilon)} \tag{7}$$

with $d(q) = \lim_{\epsilon \rightarrow 0} d(q, \epsilon)$. Due to the convexity of cumulative counts, $d(q, \epsilon)$ and $d(q)$ are non-decreasing. The probability density of finding the IR dimension d in a state is then

$$p(d, \epsilon) = \int_0^1 dq \delta(d - d(q, \epsilon)) \quad , \quad p(d) = \lim_{\epsilon \rightarrow 0} p(d, \epsilon) \tag{8}$$

If $d(q)$ is differentiable at q , then $p(d = d(q)) = 1/d'(q)$. The range of $d(q)$, equal to the support of $p(d)$, specifies the IR dimensions occurring with non-zero probability in states of interest. It is a subset of $[d_{\min}, d_{\max}]$ where

$$d_{\min} = \inf\{d \mid p(d) > 0\} \quad , \quad d_{\max} = \sup\{d \mid p(d) > 0\} \tag{9}$$

Important feature of the ensuing formalism is that

$$d_{\max} \leq d_{\text{IR}} \leq D \tag{10}$$

Here, the inequalities involving D are obvious and the last one can be most easily seen in discrete cases. Indeed, let $p(d) = \sum_{j=1}^J \mathcal{P}_j \delta(d - d_j)$ with $0 \leq d_1 < \dots < d_J \leq D$, $\mathcal{P}_j > 0$, and assume that $d_{\text{IR}} < d_J = d_{\max}$. Consider q such that $1 - \mathcal{P}_J < q < 1$. Then, $v(q, L) - v(q - \epsilon, L) = \epsilon v(q, \epsilon, L) L^{d(q, \epsilon)}$ for sufficiently small ϵ , where $\lim_{\epsilon \rightarrow 0} d(q, \epsilon) = d_J$ and $\lim_{\epsilon \rightarrow 0} \lim_{L \rightarrow \infty} v(q, \epsilon, L) = v(q) > 0$. The size of the individual $p = \epsilon / (v(q, L) - v(q - \epsilon, L))$ in this population is then $L^{-d(q, \epsilon)} / v(q, L, \epsilon)$. Hence, if $d_J < D$, then $\min\{1, Np\}$ in the definition of N_\star yields one for a sufficient L and ϵ , while if $d_J = D$, it yields $1/v(q)$. In both cases, the contribution of this population to N_\star is $\propto L^{d_J}$. Hence, $d_{\text{IR}} \geq d_J$, which contradicts the assumption and leads to (10).

3. Anderson Criticality

We now perform the dimensional analysis for critical states of $D = 3$ Anderson Hamiltonian (5) with periodic boundary conditions at the critical point $(E_c, W_c) = (0, 16.543(2))$ [23]. The calculations in Ref. [4] yielded $d_{\text{IR}} = 2.665(2) \approx 8/3$. For $d(q)$ we follow [4], keeping track of dimension defined at a finite L and extrapolating it directly. In particular,

$$d(q, \epsilon, L) = \frac{1}{\log s} \log \frac{v(q, L) - v(q - \epsilon, L)}{v(q, L/s) - v(q - \epsilon, L/s)} \tag{11}$$

with fixed $s > 1$, and $d(q, \epsilon) = \lim_{L \rightarrow \infty} d(q, \epsilon, L)$. In the analysis, we set $s = 2$. For 34 sizes in the range $16 \leq L \leq 144$, two near-zero eigenmodes were computed at 40k–100k disorder samples using the JADAMILU package [24]. We set $\epsilon = 10^{-3}$, thus splitting the interval $q \in [0, 1]$ into 1000 bins and evaluating $d(q_b, \epsilon, L)$ at $q_b = b \times 10^{-3}$, $b = 1, \dots, 1000$. We verified that this is fine enough to directly represent the $\epsilon \rightarrow 0$ limits for our purposes.

Given that, we show $d(q, L)$ at $L = 40$ and $L = 144$ in Figure 2. An important feature of the obtained behavior is the flatness in the middle part of q , indicating large probabilities for dimensions in the corresponding range. An increase of L results in a flatter $d(q, L)$ and yet a sharper range of prominent dimensions. The visible linear parts at small q mark regions where finite-size effects lead to non-convex $v(q)$. Their extent shrinks toward zero with growing L . Linearity was imposed to keep the behavior regular.

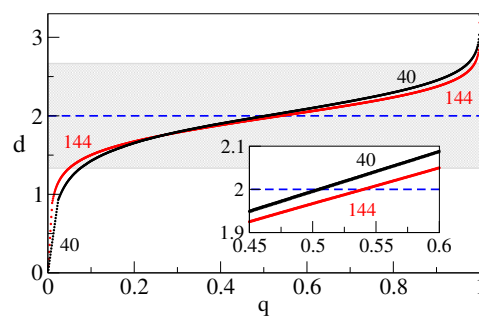


Figure 2. Function $d(q, \epsilon, L)$ at $\epsilon = 10^{-3}$ for $L = 40$ and $L = 144$ (largest) systems. Shaded region marks the range $d \in [4/3, 8/3]$.

The corresponding $p(d, L)$ obtained via (8) are shown in Figure 3. We observe sharp peaks of decreasing width, centered at $d_m \approx 2$. The error bars, too small to be visible, were

obtained via the Jackknife procedure with respect to disorder samples. The stability of d_m and its proximity to 2 is quite remarkable, as shown in the inset for the largest sizes studied. The quoted values were obtained from quadratic fits in the displayed vicinity of the maximum. The constant parts at a small d correspond to the linear segments in Figure 2.

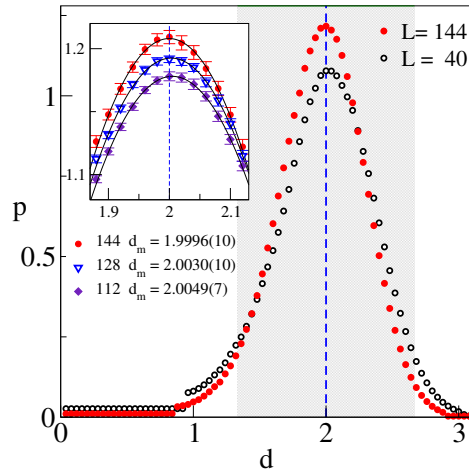


Figure 3. Function $p(d, \epsilon, L)$ at $\epsilon = 10^{-3}$ for $L = 40$ and $L = 144$ (largest) systems. Shaded region marks the range $d \in [4/3, 8/3]$.

Among the key characteristics of the dimension content $p(d)$ is its support, i.e. dimensions that can contribute to physical processes with non-zero probability density. The above properties of $p(d, L)$ imply that the support in fact spans certain $[d_{\min}, d_{\max}]$, and its specification thus reduces to finding d_{\min} and d_{\max} . To that effect, we evaluate the probabilities $p(d < d_0, L)$ of dimensions smaller than d_0 and vary d_0 upward. For each d_0 , $p(d < d_0, L)$ is the $L \rightarrow \infty$ extrapolated by fitting to a constant with general power correction. The result, shown in Figure 4 panel (a), features a probability threshold turning on near $d_0 = 1.3$. We take $d_0 = 4/3$ as a reference value: in panel (c), we show its extrapolation leading to a clean statistical zero. The analogous procedure based on $p(d > d_0)$ yields the results shown in panels (b) and (d) with $d_0 = 8/3$ referencing the other threshold.

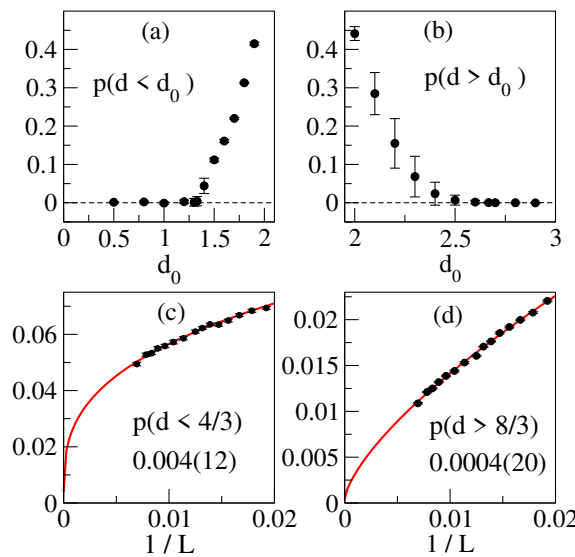


Figure 4. Probabilities $p(d < d_0)$ and $p(d > d_0)$ (panels (a,b)) in $L \rightarrow \infty$ limit. Panels (c,d) show extrapolations for $d_0 = 4/3$ and $d_0 = 8/3$.

Given the strong dominance of d_m , the second key question is whether d_m could be a discrete dimension present in Anderson critical states. This would mean that, in the $L \rightarrow \infty$

limit, $d(q, L)$ (see Figure 2) develops a strictly constant part in certain range of q . We will test this possibility for the observed $d_m = 2$ via the following procedure. Given a $d(q, L)$, we find $q_2(L)$ such that $d(q_2, L) = 2$ and calculate

$$I(\rho, L) = \int_{q_2-\rho/2}^{q_2+\rho/2} dq \left(2 - d(q, L) \right)^2 \tag{12}$$

which is only zero if $d(q, L) = 2$ on the interval. For a given ρ , we perform the $L \rightarrow \infty$ extrapolation via fit to a constant $I(\rho)$ with general power correction. Fitting data for systems with $L > 28$ leads to the results shown in Figure 5 (circles). Notice a steep decay of $I(\rho)$ with decreasing ρ , reaching $I \approx 0$ at $\rho \approx 0.4$ with errors becoming large below this point. While this could simply indicate a very steep analytic behavior of $I(\rho)$, further analysis suggests otherwise. Indeed, restricting fits to larger systems, namely $L > 32$ (diamonds) and $L > 40$ (triangles), results in an increasingly steeper decay toward zero at yet larger ρ . The natural interpretation of these tendencies is that $I(\rho) \equiv 0$ for $\rho < \rho_0 \approx 0.5$, pointing to the discrete nature of d_m .

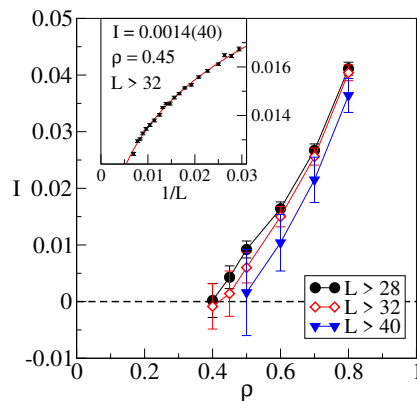


Figure 5. Function $I(\rho, L \rightarrow \infty)$ obtained by fitting in L -ranges containing increasingly larger lattices. Inset shows example of a fit in the vicinity of ρ_0 such that $I(\rho_0) \approx 0$.

The synthesis of our results suggests the following form of the spatial dimension content at the Anderson criticality

$$p(d) = \mathcal{P} \delta(d - d_m) + (1 - \mathcal{P}) \pi(d) \tag{13}$$

where $\pi(d)$ is a continuous probability distribution with support on the interval $[d_{\min}, d_{\max}]$. The parameters are

$$d_m \approx 2, \quad d_{\min} \approx 4/3, \quad d_{\max} \approx 8/3, \quad \mathcal{P} \gtrsim 1/2 \tag{14}$$

where we estimate the accuracy of d_m at the couple % and that of d_{\min}, d_{\max} at the couple %. The graphical representation of this result in terms of $d(q)$ and $p(d)$ is shown in Figure 6.

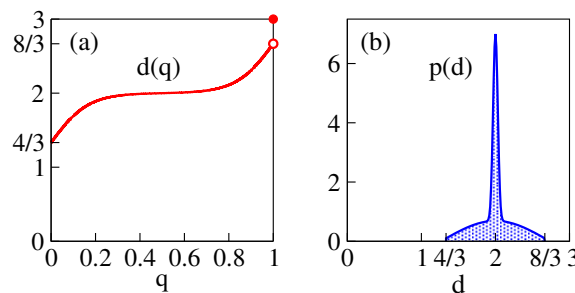


Figure 6. Schematic representation of the concluded function $d(q)$ (panel (a)) and the dimensional content $p(d)$ (panel (b)) at Anderson criticality. The narrow spike in (b) represents the δ -function.

4. Discussion

We proposed that, in addition to their measure-based effective dimension (d_{UV} or d_{IR}) [5–8], probability distributions on metric spaces can be characterized by the associated dimension content $p(d)$. The method was applied to the structure of critical states in the $D = 3$ Anderson transition (O class). Here, $p(d)$ identifies the dimensions of regions in which the electron can in fact be found, i.e. those relevant to its physics. Critical wave functions are subdimensional, multidimensional, and our new results are summarized by Equations (13) and (14). A few comments should be made.

- (i) The picture of the Anderson transition as a spatial dimension transformation (1) receives key refinements by virtue of $p(d)$. Indeed, although the critical electron is fully confined to the spatial effective support S_* of Minkowski dimension $d_{IR} \approx 8/3$ [4,9], its key substructure has $d_m \approx 2$, and the continuum of lower- and higher-dimensional features is also present. Geometrically, S_* may thus also be viewed as a surface-like structure endowed with complex lower-dimensional “hair” and higher-dimensional “halo”.
- (ii) Our results suggest that d_m is a discrete dimension and that it may assume an exact topological value of $d_m = 2$. [The mathematical meaning of “topological” in the context of IR dimension would, of course, need some clarification.] This invokes a possibility that quantum mechanics combined with pure disorder can lead to the emergence of integer dimensions. Apart from an understanding of Anderson transitions, variations on such dynamics could find relevance in modeling an emergent space in the early universe. A more detailed description of this geometry would be needed.
- (iii) The connection between d_{IR} and $p(d)$ results from the built-in additivity that makes both measure-based: in the case of d_{IR} it is the additivity of effective counting with respect to combining the systems [5,6], and in the case of $d(q)$ the familiar additivity of ordinary counting. This aspect is key to the interpretation of these concepts as spatial dimensions. Indeed, it is because the Hausdorff measure and the Minkowski count properly quantify volume that dimensions based on them became useful and accepted characteristics of space.
- (iv) It is natural to ask whether some features of the described spatial structure have analogues in the multifractal approach [16,17] adopted to the IR Anderson setting via the moment method [25]. Here the focus is on the so-called dimensional spectrum $f(\alpha)$. Inner workings of the method give special status to the information dimension [26] in a way somewhat similar to d_m . It would be interesting to study the possible association between the two in detail. (See also the debate regarding d_{IR} in Refs. [27–29].)
- (v) Our data are consistent with critical wave functions being of proper dimension ($d_{IR} = d_{max}$). However, albeit state of the art, their statistical power is not sufficient to reach a sharper conclusion at this point.
- (vi) Our findings acquire another angle in light of recent results [7,30] in quantum chromodynamics (QCD). The original proposal that the Anderson-like mobility edge $\lambda_A > 0$ appears in the QCD Dirac spectrum upon thermal chiral transition [31,32], worked out by Refs. [33–35], became more structured. Indeed, the existence of a new mobility edge $\lambda_{IR} \equiv 0$ has been concluded, and its simultaneous appearance with λ_A at temperature T_{IR} was conjectured [30]. Here T_{IR} marks the transition to a phase featuring the IR scale invariance of glue fields [36]. The approach to IR criticality ($\lambda \rightarrow \lambda_{IR}^+$) was found to proceed via $d_{IR} \approx 2$ Dirac modes [7], with the topological origin of the dimension suspected. Clarifying a possible relation of this to $d_m \approx 2$ found here may shed new light on the QCD–Anderson localization connection.
- (vii) The proposed IR/UV guises of multidimensionality formalism easily extend to more general situations without the metric. Here the sequence $\{O_k\}$ involving collections $O_k = (o_{k,1}, o_{k,2}, \dots, o_{k,N_k})$ with an increasing number N_k of arbitrary objects comes with the associated sequence $\{P_k\}$ of the relevance (probability) vectors. The role of d_{IR} and d_{UV} is taken by the effective counting dimension $0 \leq \Delta \leq 1$ defined via scaling $N_*[P_k] \propto N_k^\Delta$ for $k \rightarrow \infty$ [8]. The dimension function $d(q)$ is replaced by an analogous

$\gamma(q)$ and the dimension content $p(d)$ by $p(\gamma)$. The target ($k \rightarrow \infty$) effective collection defined by $\{O_k\}, \{P_k\}$ is then

$$\begin{aligned} & \text{subdimensional if} && \Delta < 1 \\ & \text{multidimensional if} && p(\gamma) \neq \delta(\gamma - \gamma_{\max}) \\ & \text{of proper dimension if} && \Delta = \gamma_{\max} \end{aligned} \quad (15)$$

where $\gamma_{\max} = \sup \{\gamma \mid p(\gamma) > 0\}$ and $\gamma_{\max} \leq \Delta$.

Author Contributions: Conceptualization, I.H.; methodology, I.H.; software, P.M.; validation, I. H. and P. M.; formal analysis, I.H. and P.M.; investigation, I.H. and P.M.; resources, P.M.; data curation, P.M.; writing original draft, I.H.; writing review & editing, I.H. and P.M. .; visualization, P.M. All authors have read and agreed to the published version of the manuscript.

Funding: P.M. was supported by the Slovak Grant Agency VEGA, Project n. 1/0101/20.

Institutional Review Board Statement: Not applicable.

Data Availability Statement: The numerical data presented here is available upon request.

Conflicts of Interest: The authors declare no conflict of interest.

References

- Anderson, P.W. Absence of Diffusion in Certain Random Lattices. *Phys. Rev.* **1958**, *109*, 1492. [CrossRef]
- Schenk, O.; Bollhöfer, M.; Römer, R.A. On Large-Scale Diagonalization Techniques for the Anderson Model of Localization. *SIAM Rev.* **2008**, *50*, 91–112. Available online: <http://www.jstor.org/stable/20454065> (accessed on 15 October 2023). [CrossRef]
- Abrahams, E.; Anderson, P.W.; Licciardello, D.C.; Ramakrishnan, T.V. Scaling Theory of Localization: Absence of Quantum Diffusion in Two Dimensions. *Phys. Rev. Lett.* **1979**, *42*, 673. [CrossRef]
- Horváth, I.; Markoš, P. Super-Universality in Anderson Localization. *Phys. Rev. Lett.* **2022**, *129*, 106601. [CrossRef] [PubMed]
- Horváth, I.; Mendris, R. Effective Number Theory: Counting the Identities of a Quantum State. *Entropy* **2020**, *22*, 1273. [CrossRef]
- Horváth, I. The Measure Aspect of Quantum Uncertainty, of Entanglement, and the Associated Entropies. *Quantum Rep.* **2021**, *3*, 534–548. [CrossRef]
- Alexandru, A.; Horváth, I. Unusual Features of QCD Low-Energy Modes in the Infrared Phase. *Phys. Rev. Lett.* **2021**, *127*, 052303. [CrossRef]
- Horváth, I.; Markoš, P.; Mendris, R. Counting-Based Effective Dimension and Discrete Regularizations. *Entropy* **2023**, *25*, 482. [CrossRef]
- Horváth, I.; Markoš, P. Low-dimensional life of critical Anderson electron. *Phys. Lett. A* **2023**, *467*, 128735. [CrossRef]
- Aoki, H. Critical behaviour of extended states in disordered systems. *J. Phys. Solid State Phys.* **1983**, *16*, L205. [CrossRef]
- Soukoulis, C.M.; Economou, E.N. Fractal Character of Eigenstates in Disordered Systems. *Phys. Rev. Lett.* **1984**, *52*, 565. [CrossRef]
- Castellani, C.; Peliti, L. Multifractal wavefunction at the localisation threshold. *J. Phys. Math. Gen.* **1986**, *19*, L429. [CrossRef]
- Evangélou, S.N. Multifractal wavefunctions at the mobility edge. *J. Phys. Math. Gen.* **1990**, *23*, L317. [CrossRef]
- Schreiber, M.; Grussbach, H. Multifractal wave functions at the Anderson transition. *Phys. Rev. Lett.* **1991**, *67*, 607. [CrossRef] [PubMed]
- Janssen, M. Multifractal analysis of broadly-distributed observables at criticality. *Int. J. Mod. Phys. B* **1994**, *8*, 943. [CrossRef]
- Falconer, K. *Fractal Geometry: Mathematical Foundations and Applications*, 3rd ed.; Wiley: Hoboken, NJ, USA, 2014.
- Halsey, T.C.; Jensen, M.H.; Kadanoff, L.P.; Procaccia, I.; Shraiman, B.I. Fractal measures and their singularities: The characterization of strange sets. *Phys. Rev. A* **1986**, *33*, 1141. [CrossRef]
- Mildenberger, A.; Evers, F.; Mirlin, A.D. Dimensionality dependence of the wave-function statistics at the Anderson transition. *Phys. Rev. B* **2002**, *66*, 033109. [CrossRef]
- Vasquez, L.J.; Rodriguez, A.; Römer, R.A. Multifractal analysis of the metal-insulator transition in the three-dimensional Anderson model. I. Symmetry relation under typical averaging. *Phys. Rev. B* **2008**, *78*, 195106. [CrossRef]
- Rodriguez, A.; Vasquez, L.J.; Römer, R.A. Multifractal analysis of the metal-insulator transition in the three-dimensional Anderson model. II. Symmetry relation under ensemble averaging. *Phys. Rev. B* **2008**, *78*, 195107. [CrossRef]
- Rodriguez, A.; Vasquez, L.J.; Slevin, K.; Römer, R.A. Multifractal finite-size scaling and universality at the Anderson transition. *Phys. Rev. B* **2011**, *84*, 134209. [CrossRef]
- Ujfalusi, L.; Varga, I. Finite-size scaling and multifractality at the Anderson transition for the three Wigner-Dyson symmetry classes in three dimensions. *Phys. Rev. B* **2015**, *91*, 184206. [CrossRef]
- Slevin, K.; Ohtsuki, T. Critical Exponent of the Anderson Transition Using Massively Parallel Supercomputing. *J. Phys. Soc. Jpn.* **2018**, *87*, 094703. [CrossRef]

24. Bollhöfer, M.; Notay, Y. JADAMILU: A software code for computing selected eigenvalues of large sparse symmetric matrices. *Comput. Phys. Commun.* **2007**, *177*, 951–964. [[CrossRef](#)]
25. Evers, F.; Mirlin, A.D. Anderson transitions. *Rev. Mod. Phys.* **2008**, *80*, 1355. [[CrossRef](#)]
26. Grassberger, P. Generalizations of the Hausdorff dimension of fractal measures. *Phys. Lett. A* **1985**, *107*, 101–105. [[CrossRef](#)]
27. Burmistrov, I.S. Comment on “Super-Universality in Anderson Localization”. *Phys. Rev. Lett.* **2023**, *131*, 139701. [[CrossRef](#)] [[PubMed](#)]
28. Horváth, I.; Markoš, P. Horváth and Markoš Reply. *Phys. Rev. Lett.* **2023**, *131*, 139702. [[CrossRef](#)]
29. Horváth, I.; Markoš, P. Response to Comment on “Super-universality in Anderson localization”. *arXiv* **2022**, arXiv:2212.02912.
30. Alexandru, A.; Horváth, I. Anderson metal-to-critical transition in QCD. *Phys. Lett. B* **2022**, *833*, 137370. [[CrossRef](#)]
31. Garcia-Garcia, A.M.; Osborn, J.C. Chiral phase transition and Anderson localization in the instanton liquid model for QCD. *Nucl. Phys. A* **2006**, *770*, 141–161. [[CrossRef](#)]
32. Garcia-Garcia, A.M.; Osborn, J.C. Chiral phase transition in lattice QCD as a metal-insulator transition. *Phys. Rev. D* **2007**, *75*, 034503. [[CrossRef](#)]
33. Kovacs, T.G.; Pittler, F. Anderson Localization in Quark-Gluon Plasma. *Phys. Rev. Lett.* **2010**, *105*, 192001. [[CrossRef](#)] [[PubMed](#)]
34. Giordano, M.; Kovacs, T.G.; Pittler, F. Universality and the QCD Anderson Transition. *Phys. Rev. Lett.* **2014**, *112*, 102002. [[CrossRef](#)] [[PubMed](#)]
35. Ujfalusi, L.; Giordano, M.; Pittler, F.; Kovács, T.G.; Varga, I. Anderson transition and multifractals in the spectrum of the Dirac operator of quantum chromodynamics at high temperature. *Phys. Rev. D* **2015**, *92*, 094513. [[CrossRef](#)]
36. Alexandru, A.; Horváth, I. Possible new phase of thermal QCD. *Phys. Rev. D* **2019**, *100*, 094507. [[CrossRef](#)]

Disclaimer/Publisher’s Note: The statements, opinions and data contained in all publications are solely those of the individual author(s) and contributor(s) and not of MDPI and/or the editor(s). MDPI and/or the editor(s) disclaim responsibility for any injury to people or property resulting from any ideas, methods, instructions or products referred to in the content.